Provenance Identification of the Inkslab Unearthed from Liangfu Gao's Grave of the Song Dynasty (960-1279 CE) in Chengdu, Sichuan, China

Tongyang Wang
College Civil Engineering and Mechanics, Lanzhou University https://orcid.org/0000-0003-3682-758X
Yangmin Gong
Chengdu Institute of Cultural Relics and Archaeology
Shiming Wang (shimingw@swjtu.edu.cn)
Southwest Jiaotong University
Lin Xiao
Chengdu Institute of Cultural Relics and Archaeology
Tao Yang
Chengdu Institute Relics and Archaeology

Research article

Keywords: Archaeology of science and technology, inkslab, Song Dynasty, Provenance, Mineralogical analysis, Geochemical element analysis

Posted Date: December 3rd, 2020

DOI: https://doi.org/10.21203/rs.3.rs-117511/v1

Abstract

In order to infer the provenance of ancient inkslab excavated from Liangfu Gao's Grave of the Song dynasty (960-1279 CE) in Chengdu, a multi-analytical approach, including polarizing microscope, scanning electron microscope (SEM), X-ray powder diffraction (XRD), energy dispersive spectroscopy (EDS), X-ray fluorescence (XRF), inductively coupled plasma-atomic emission spectrometry (ICP-AES) and inductively coupled plasma mass spectrometry (ICP-MS) was used for the complete characterization of the ancient inkslab and the collected sample materials of this inkslab. The comparison of the results about mineral structure, major, trace and rare earth elements (REE) suggested that this unearthed inkslab of Song dynasty was Pu inkslab, which was famous in Pujiang County of Chengdu, and conjectured that its particular structure made it show the good inking performance. This work provided a reliable basis for the study of the historical and cultural inheritance of the Gao family, providing more direct evidence for the produce and development of the inkslab in the Song Dynasty.

1. Introduction

The inkslab is one of the traditional Chinese "Four Treasures of the Study". It shows a strong cultural attribute, developed with the prosperity of ancient Chinese culture. In 2018, a beautiful inkslab (as shown in Fig. 1) was unearthed in the tomb of No. 17 at the Gao family tomb of the Song Dynasty in Damian Town, Chengdu, China. It was 18.2 cm long, 12 cm wide, 2.5 cm high, and the whole inkslab was grayish green. Its surface was left with black flakes, suspected ink marks. Therefore the inkslab may have been used by the tomb's occupant when he was alive. According to the unearthed epitaph materials, the occupier of No. 17 tomb was named Liangfu Gao, and he was the grandson of Keming Gao who was a famous landscape painter of the northern Song dynasty for his extremely high painting achievements. Until now, Keming Gao's paintings were treasured by the Metropolitan Museum of Art. Hence, the discovered inkslab provided significant material information for studying the development of the profound painting and calligraphy art of the Gao family, and also provided an important basis for studying the development of social culture and art in the Song Dynasty of China. However, the analysis of the provenance of this inkslab is the key to the study about the cultural exchange and the circulation of inkslab mining in Song dynasty, which is of great academic significance.

The study on the provenance of unearthed cultural relics helps us to understand the ancients' ways and means to obtain resources, to a certain extent, it also reflects the resource strategies behind their substance transactions and cultural exchanges, their influence on the process of civilization development [1, 2]. Traditional archeologists' research on the origin of unearthed cultural relics is mainly based on shape, decoration and the cultural connotation behind it. However, these methods are closely related to the subjective factors such as personal knowledge level and experience [3]. Since Wocel first proposed in the 1850s that the age and provenance of cultural relics might be related to their chemical composition, many scientists began to test the chemical composition of cultural relics with modern scientific and technological means, trying to use them as one of the main scientific evidences for the identification of cultural relics [4]. Spectrometric analysis by using scientific methods is a powerful and more necessary

tool to place unearthed historical artifacts in their real historical context and to avoid any controversy regarding their origin [5].

Among them, rare earth elements such as Th, Sc, Cr and Co are the most valuable for the analysis of source area characteristics because of their slightly solubility, which show the relative stability. These elements are only transported with the terrigenous clastic sediments, so they can reflect the geochemistry of source area [6]. M. emami et al. determined the mineral and chemical composition of these stones and their source by REE analysis of the building materials of the stele built in Pasargadae [7]. Zhang Yuyan et al. analyzed the mineral composition and REE of nephrite in the new period of Gansu province, and discussed its origin via XRD, LA-ICP-MS and other analytical methods [8]. Wen et al. attempted to test the validity of the signatures of REE as a tool to judge the effect of diagenesis on fossil teeth [9]. In 2012, Vincenzo Ferrini et al. investigated the provenance of archaeological carved slabs of the Langobard art in churches of Peligna Valley and Spoleto (Italy) through a multi-analytical approach, including petrographic characterization, chemical, carbon and oxygen isotope composition [10]. Wei et al. revealed the foundry area of bronze vessels according to the REE analysis [11]. Therefore, chemical element analysis could be one of the effective methods for the study of cultural relics.

Here, we attempted to discuss the Mineral structure and geochemical characteristics of inkslab and synthetically judged the provenance of its raw materials and the mechanism of ink formation.

2. Methods And Materials

2.1. Material background

The ancients were extremely careful about the selection of materials when making inkslab. Generally, the stone used as inkslab should be sedimentary rock or metamorphic rock with larger thickness [12]. This special material selection method provided a reliable basis for the study of raw material origin. It was speculated that the inkslab may be Pu inkslab made in Sichuan according to its color, shape characteristics and the place of its discovered. Pu inkslab was the famous traditional inkslab in China. Its name was called Pu because it was carved by Pu stone and came from Yan Jinggou in Sichuan Province. Up to now, there is still a place called “Pu Inkslab Village” in Heshan town, Pujiang country, where the Pu inkslab was abundant in the past. If this unearthed inkslab could be determined to be made of Pu stone, it will provide important physical evidence for the historical research of Pu inkslab.

2.2 Geological characteristics of Pu stone producing area

Pu stone was mined in the upper part of Xu Jiahe group of Triassic in Xiongpo anticline (T_3xj^2), which is a coal-bearing deposit of the River-Lake and marshes (as shown in Fig. 2A). Xu Jiahe Formation was named after Xu Jiahe Village, Gongnong Town, North Guangyuan City [13]. It mainly refers to a set of strata with a combination of yellow-gray pebbled sandstone, sandstone, siltstone and mudstone intercalated coal seam from Norian to Rhaetian of Late Triassic. The deposit is thick and can reach thousands of meters. In the vertical section, sandstone and mudstone often form unequal thickness

rhythm layers dominated by sandstone. The upper layer is composed of massive conglomerate, which is hundreds of meters to nearly kilometers thick and rich in plants and bivalves fossils [14]. According to the historical materials of the Qing Dynasty “Pujiang county annals” recorded that “Pu stone in the Xiangshui River area was the top grade of all raw materials”. The lithology of the Xu Jiahe group in the Xiangshui River area is composed of moderately and thickly stratified quartzite siltstone, mainly gray and yellow-gray, which includes the mudstone and coal line. (as shown in Fig. 2B).

2.3 Analytical methods

Smaller fragments from unearthed inkslab were selected as sample 1 and called relics sample (as shown in Fig. 1). Five samples were collected from the upper section of Xu Jiahe group (T_3xj^2) according to the color and grain size of sample 1, which were called samples 2, 3, 4, 5, 6 (samples 2–6), respectively (as shown in Fig. 1). They were served as the control groups and temporarily used to be the "source rock" of inkslab for matching analysis. The matching analyses mainly include phase analysis, microstructure observation, determination of the major element, trace element and rare earth element. Among them, microstructure was observed by polarizing microscope, SEM and EDS. The major element were measured by XRF, and the trace element, REE were measured by ICP-AES and ICP-MS, respectively.

3. Results And Discussion

3.1 Mineral structure characterization

- *Polarizing microscope characterization.* As shown in Fig. 3, the control samples were thin layer of siltstone with multiple strip. Their touch feeling of surface and color were similar to the unearthed relics sample, which was grayish-green. Besides, the surface were wavy and uneven with visibly horizontal layer. It could be seen that samples 1–6 were composed of silt-grade crumb, and showed their basic skeleton via the polarizing microscope. The sorting of the clastic particles was moderate, and the roundness was not well. The Fig. 3 also indicated that mineral particles minerals contained quartz, sericite, chlorite and other minerals. They showed directionality, and their plastic deformation was caused by compaction [15].

- *XRD characterization.* Figure 4 showed the XRD patterns of relics sample No.1 and control samples No. 2, 3, 4, 5, 6. It exhibited diffraction peaks at 2θ along 27.1, 29.2 corresponding to the sericite. It could be seen that there are common diffraction peaks at 2θ along 12.6, 25.7, which belong to chlorite. In addition, diffraction peaks at 2θ along 21.2, 36.9 were consistent with the quartz [16]. The XRD results demonstrated that the mineral types of the cultural relics samples are identical with the control samples.

- *SEM and EDS characterization.* Firstly, the surfaces of samples were sprayed with gold before testing. Then their microstructures were observed by SEM (Fig. 5) and the distributions of chemical elements on their surfaces were obtained through EDS (Fig. 6). On the one hand, it was found that both the relic sample and the control samples mostly showed micro-squama textures, mainly

containing elements such as Si, O, Al, Fe, K, Ca, C, Na, etc., and Si, O, Al elements were absolutely dominant. On the other hand, the compositions of samples suggested that inkstones mainly consist of Oxygen-containing silicate minerals, aluminosilicate minerals, and the intergranular pores are filled with carbonate minerals and clay minerals. Among them, the morphology of minerals were mainly composed of irregular flaky (such as goeschwitzite, mixed-layer illite/smectite) and thin flaky (such as montmorillonite), with fuzzy boundary and scattered distribution.

In addition, the SEM images suggested that there were many lamellar minerals on the inkslab surface and they were squama-like (Fig. 5) [17, 18]. As shown in Fig. 6, after superimposing individual elements through the EDS surface scanning, it was concluded that such minerals are mostly silicate minerals (quartz, sericite, chlorite, etc.). These minerals were arranged together, such as "blade" obliquely standing on the inkstone surface, known as “inkslab blade” [19, 20]. When grinding the ink, moving of the ink on the inkslab surface could be cut continuously by the inkslab blade to effectively meet the requirements of generating ink. Moreover, the arrangement of the fragment not only made the ink fine and symmetrical, but also effectively protected the inkslab and made the surface durable. Besides, irregular plate-like clay minerals between the minerals played a role in cementation, which not only ensured the strength requirements of the inkslab, but also made the surface smooth and mild.

3.2 Chemical element characterization

- *XRF characterization.* The major elements reflect the chemical composition and relative content of the minerals that make up the stones. In addition, the characteristics of the major elements show the overall properties of the rock [21]. The data results for the major elements were given in Table 1.

Table 1
Major (mass %) elements of relics sample (1) and control samples (2, 3, 4, 5, 6)

Chemical composition	1	2	3	4	5	6
SiO_2	64.38	58.14	57.80	53.09	61.75	63.65
Al_2O_3	15.68	15.86	16.08	20.37	14.04	13.18
MgO	2.17	2.35	2.33	2.58	2.07	1.90
CaO	0.38	4.17	4.65	2.41	4.55	4.73
TFe_2O_3	7.09	7.15	6.52	7.10	5.93	5.02
TiO_2	0.81	0.71	0.70	0.84	0.67	0.64
Na_2O	0.85	0.30	0.17	0.12	0.67	0.62
K_2O	3.24	2.97	3.17	4.13	2.42	2.18
LOI(1000 ℃)	4.49	7.91	8.18	8.97	7.65	7.57
∑	99.09	99.38	99.6	99.61	99.75	99.49

There were many existential forms of iron element, and the TFe_2O_3 mainly included Fe_2O_3 and FeO. However, the content largely influenced by the material provenance. Additionally, aluminum, sodium and potassium were mainly found in clay minerals mica and other minerals. It was found that Al_2O_3 mainly existed in the crystal voids in the form of clay minerals via the EDS (Fig. 6) [22]. The chemical composition of major elements was presented in Table 1. In Fig. 7 are plotted the contents of major elements of the archaeological sample (1) and control samples. On the whole, the main elements of the two groups of samples have similar change rules, and quartz is taken as the main framework of rock, which is consistent with the observation results of polarizing microscope. In addition, the relics sample of contents of Al_2O_3, MgO, TFe_2O_3, TiO_2 and K_2O were all in the change ranges of the corresponding control group [23]. The ratio of Al_2O_3 and SiO_2 (Al_2O_3/SiO_2) represented the ratio of all aluminum-containing minerals (mica, clay minerals, etc.) to quartz [24, 25]. Therefore, the calculation results showed that the Al_2O_3/SiO_2 of the relics sample was 0.24, while ranges of the control groups was 0.21 ~ 0.38 with an average of 0.27. The relics samples were in the variation range of the control group and close to the average value, indicating that the correlations were consistent between the aluminum-containing minerals and quartz. In a word, it is concluded that the cultural relics samples are well matched with the control samples from the perspective of major elements.

- *ICP-AES and ICP-MS characterization.* What's more, in order to avoid the experimental error caused by rock weathering, trace elements and rare earth elements were analyzed. The trace elements and rare earth elements are relatively stable and have high homogenization characteristics, which determines that they can provide relatively accurate geochemical parameters for sedimentological provenance analysis. Incompatible elements, such as La, Zr, Hf, Co, Sc, Nb, Th (inert elements), show stable properties under various geological processes of surface and are less or not affected by the deposition process. Despite the transformation effect during the deposition process, geochemistry is still dominated by provenance, which is used as an indicator of the composition characteristics of crop sources. During the process of practice apply, a more stable ratio of trace elements (La/Sc, La/Co, Th/Sc, Th/Co, Th/Cr) is often adopted to indicate the source stability instead of the absolute values in order to exclude the influence of particle size and other factors. The data results of trace and rare earth elements were listed in Table 2.

Table 2
Contents of trace, rare earth (μg/g) elements in relics sample (1) and control samples (2, 3, 4, 5, 6)

element	1	2	3	4	5	6
La	39.4	36.4	36.3	48.4	34.4	34.9
Ce	79.0	73.8	72.7	97.1	70.4	71.5
Pr	9.10	8.23	8.54	10.65	7.94	8.29
Nd	34.8	32.8	33.2	39.3	31.4	32.9
Sm	6.61	6.21	6.47	6.85	6.35	6.90
Eu	1.27	1.40	1.37	1.44	1.26	1.52
Gd	5.16	5.23	5.82	5.03	5.17	6.24
Tb	0.90	0.92	0.87	0.85	0.83	0.85
Dy	4.67	4.75	4.88	4.53	4.51	4.77
Ho	1.00	0.99	1.08	0.97	0.96	1.06
Er	2.65	3.02	3.06	2.84	2.52	2.71
Tm	0.42	0.44	0.46	0.45	0.40	0.43
Yb	2.77	2.80	3.01	3.02	2.51	2.55
Lu	0.39	0.42	0.45	0.44	0.35	0.36
Rb	144.0	139.0	153.5	198.0	116.0	105.0
Ba	432	487	599	656	400	412
Th	14.00	13.50	13.70	17.50	12.20	12.00
U	3.01	3.24	3.20	4.04	2.74	2.74
Nb	14.1	13.4	13.7	16.2	12.6	12.2
Ta	1.00	0.98	0.90	1.08	0.84	0.82
La	39.40	36.40	36.30	48.40	34.40	34.90

LREE = La + Ce + Pr + Nd + Sm + Eu
HREE = Gd + Tb + Dy + Ho + Er + Tm + Yb + Lu + Y
∑REE = LREE + HREE
δEu = EuN/ (SmN + GdN)*2
δCe = Ce / (LaN + PrN)*2)

element	1	2	3	4	5	6
Ce	79.00	73.80	72.70	97.10	70.40	71.50
Co	15.20	14.10	54.70	22.80	10.00	15.80
Cr	77	84	91	113	73	64
Pb	55.8	24.8	93.9	57.3	20.7	23.7
Pr	9.10	8.23	8.54	10.65	7.94	8.29
Sr	59.70	136.00	152.00	110.00	144.00	159.00
Nd	34.80	32.80	33.20	39.30	31.40	32.90
Zr	201.00	172.00	176.00	175.00	181.00	197.00
Hf	5.70	4.70	4.50	4.60	4.70	4.70
Sc	12.50	14.00	13.80	16.30	11.50	10.40
Sm	6.61	6.21	6.47	6.85	6.35	6.90
Eu	1.27	1.40	1.37	1.44	1.26	1.52
Ti	4855.95	4256.45	4196.5	5035.8	4016.65	3836.8
Gd	5.16	5.23	5.82	5.03	5.17	6.24
Tb	0.90	0.92	0.87	0.85	0.83	0.85
Dy	4.67	4.75	4.88	4.53	4.51	4.77
Yb	2.77	2.80	3.01	3.02	2.51	2.55
Y	26.7	28.6	30.1	28.1	28.0	28.6
Ho	1.00	0.99	1.08	0.97	0.96	1.06
Er	2.65	3.02	3.06	2.84	2.52	2.71
Zr	201.00	172.00	176.00	175.00	181.00	197.00
∑REE	188.14	177.41	178.21	221.87	169.00	174.98
LREE	170.18	158.84	158.58	203.74	151.75	156.01

LREE = La + Ce + Pr + Nd + Sm + Eu

HREE = Gd + Tb + Dy + Ho + Er + Tm + Yb + Lu + Y

∑REE = LREE + HREE

δEu = EuN/ (SmN + GdN)*2

δCe = Ce / (LaN + PrN)*2)

element	1	2	3	4	5	6
HREE	17.96	18.57	19.63	18.13	17.25	18.97
LREE/HREE	9.48	8.55	8.08	11.24	8.80	8.22
La_N/Yb_N	1.34	1.23	1.14	1.51	1.29	1.29
δEu	1.02	1.15	1.05	1.15	1.03	1.09
δCe	0.99	1.01	0.98	1.01	1.01	1.00
La/Co	2.59	2.58	0.66	2.12	3.44	2.21
La/Sc	3.15	2.60	2.63	2.97	2.99	3.36
Th/Sc	1.12	0.96	0.99	1.07	1.06	1.15
Th/Co	0.92	0.96	0.25	0.77	1.22	0.76
Th/Cr	0.18	0.16	0.15	0.15	0.17	0.19
LREE = La + Ce + Pr + Nd + Sm + Eu						
HREE = Gd + Tb + Dy + Ho + Er + Tm + Yb + Lu + Y						
∑REE = LREE + HREE						
δEu = EuN/ (SmN + GdN)*2						
δCe = Ce / (LaN + PrN)*2)						

The Primitive-mantle normalized incompatible element diagrams of samples 1–6 were shown in Fig. 8b. It could be seen that the results of relics sample (1) obtained in this study for most of the elements, such as Nb□Ta□Zr□Hf, are in good agreement with the positions overlap of control samples (2,3,4,5,6), indicating the similar overall characteristics between relics samples and the control samples [26, 27]. The calculated ratios of La/Sc (2.60 ~ 3.36), La/Co (0.66 ~ 3.44), Th/Sc (0.96 ~ 1.15), Th/Co (0.25 ~ 1.22) and Th/Cr (0.15 ~ 0.19) in Table 2 illustrated the source stability of samples 1–6, with the average of 2.91, 2.20, 1.05, 0.79 and 0.16 for each other. Obviously, the trace element ratios of the cultural relic sample 1 and control groups 2–6 were similar, and the average values of the former was close to the latter.

According to previous studies, the main factor controlling REE composition in sediments is provenance [28]. Therefore, the characteristics of REE partition model curve are one of the reliable indicators for provenance analysis [29]. The standardization of REE used in different rock types is distinguishing. North American Shales (NASC) could better reflect the geochemical characteristics of sedimentary rocks than other standardization. In this study, NASC was used as the standard to standardize the data of REE in sample 1–6 and the NASC standardized partition pattern of REE was obtained Fig. 8a [30]. The

normalized REE patterns indicated that the overall correlation of samples 1–6 is consistent, and the regularity is evident, without the separation of curves. The control samples 2–6 were characterized by ∑REE, LREE and HREE contents (the average content being 184.29, 165.78 and 18.51, severally) [31, 32]. The results proved that changes of ∑REE, LREE and HREE contents were 169 ~ 221.87, 151.75 ~ 203.74 and 17.25 ~ 19.63, respectively.

As can be seen from Table 2, the average values of ∑REE, LREE and HREE of samples 1–6 were higher than the NASC standard values. Among them, sample 1 and samples 2–6 showed a similar trend, and the former was within the range of the latter [33, 25]. On one hand, the higher the LREE/HREE value is, the more concentrated the LREE are, while the HREE are relatively scarce [33, 34]. On the other hand, La_N/Yb_N value is the slope of the distribution curve in the standardized diagram of REE, showing the degree of inclination of the curve. When the La_N/Yb_N value exceeds 1 or not, the curve inclines toward the right or left, which belongs to LREE concentrated type or LREE deficit type; when the value is equal to 1, the curve is horizontal [35]. Higher REE concentrations suggested that the dominant REE carrier phase might be a detrital mineral, which was consistent with the results of SEM characterization [36–38]. There is a consistent value of about 1.34, 1.23, 1.14, 1.51, 1.29, 1.29 for La_N/Yb_N and LREE/HREE ratios for samples 1–6, indicating a slight LREE enrichment in relation to the average shale NASC [39].

Besides, δEu and δCe values, the third geochemical indices, were used to illustrate the degree of Eu-anomaly and Ce-anomaly [40, 41]. The consistent values of samples 1–6 about 1.03 ~ 1.15 for δEu and 0.98 ~ 1.01 for δCe (Table 2), indicating positive anomaly of Eu and no anomaly for Ce, which also suggesting the similar degree of anomaly between relics sample (1) and control samples (2,3,4,5,6) [42]. As the above discussions, the relics sample 1 and the control samples 2–6 exhibited strong identities from the aspects of slope the distribution-curve slope, differential degree and degree of differentiation and deficit degree. It could be demonstrated that the unearthed inkslab and the control samples come from the same geological provenance.

4. Conclusion

Geochemical characteristics, could provide qualitative and quantitative information about the provenance of the unearthed inkslab, avoiding researchers' subjective factors. Meanwhile, the mineral structural characteristics made the conclusion more reliable. This work first demonstrated that the inkslab unearthed in the tomb of Song dynasty was Pu inkslab, and conjecture that its particular structure made it show the good inking performance. Additionally, Gao family, as one of the most famous families in Sichuan during the period of the Song dynasty, took Pu inkslab as daily stationery and burial objects, demonstrating that Pu inkslab was popular and its trade flow was very convenient at that time.

The significance of this work was that not only provided precious objective information for the Pu inkslab and enriched its historical evolution, but, more importantly, explored potential cultural information of the value might be underestimated nowadays. Overall, the combination of archaeology and geochemistry will

form an effectively analytical method and provide a choice for infer the provenance of other precious culture heritages.

Abbreviations

CE: Common Era; REE: rare earth elements; LREE: light rare earth elements; HREE: heavy rare earth elements; SEM: scanning electron microscope; XRD: X-ray powder diffraction; EDS: energy dispersive spectroscopy; XRF: X-ray fluorescence; ICP-AES: inductively coupled plasma-atomic emission spectrometry; ICP-MS: inductively coupled plasma mass spectrometry; LOI: loss on ignition; NASC: North American shales.

Declarations

Authors' contributions

TW carried out the experiments and drafted the manuscript. YG conducted the excavation and supplied archaeological data for the tomb. SW designed research and proofread the manuscript; LX and TY provided support and contributed to data analysis and processing. All authors read and approved the final manuscript.

Acknowledgements

We are grateful to Qibin He (secretary of Pu inkslab Village Party Branch) and Qingliang Lai (the inheritor of intangible cultural heritage) for sharing their knowledge about Pu inkslab and Pu stone, kindly inviting us for field investigations. We also like to thank Prof. Jianli Chen from Peking University, Prof. Li Li from Chinese Academy of Cultural Heritage and Ir. Zhizhong Hu from Chengdu Center of China Geological Survey for their invaluable help and advice in this work. Lastly, thanks to the editor and reviewers who had given us many great suggestions on this paper.

Availability of data and materials

All data generated or analyzed during this study are included in this published article.

Competing interests

The authors declare that they have no competing interests.

Funding

The research described in this paper was financially supported by the Natural Science Foundation of China (Grant Nos. 41202042 and 41272079).

References

1. Fossati S, Pesce GLA, Decri, A. Provenance Study of Wood Found in Archaeological and Architectural Objects. Proceedings of the 37th International Symposium on Archaeometry. 2008. p.405-409.
2. Tripati S, Mudholkar A, Vora K H, Rao BR, Gaur AS, Sundaresh. Geochemical and mineralogical analysis of stone anchors from west coast of India: provenance study using thin sections, XRF and SEM-EDS. J Archaeol Sci. 2010;37:1999-2009.
3. Wei G, Qin Y, Hu Y, Huang F, Xu T, Wang C. Provenance tracking of Bronze Vessel Using Rare Earth Elements in Clay Mould Residues. Rock and Mineral Anal. 2007;26:145-149.
4. Zhou S, Fu L, Leung B. Study on the Cultural Relic Material Site and Period by EDXRF. Spectrosc Spect Anal. 2008;28:1181-1185.
5. Fayçal K, Boudraa L, Benabdelghani I, Bououden M. TL dating and XRF clay provenance analysis of ancient brick at Cuicul Roman city, Algeria. J Radioanal Nucl Ch. 2019;320:395-403.
6. Grunsky E, Massey N. Using geochemical data: Evaluation, presentation, interpretation. Comput Geosci. 1995;21:439-441.
7. Emami M, Eslami M, Fadaei H, Karami HR, Ahmadi K. Mineralogical-Geochemical Characterization and Provenance of the Stones Used at the Pasargadae Complex in Iran: A New Perspective. Archaeometry. 2018;60:1184-1201.
8. Zhang Y, Qiu Z, Yang J, Zhang Y, Yang H, Yang J, et al. The geological and geochemical characteristics of nephrites in Maxianshan, Gansu province and their implication for raw material source of the Qijia Culture jadewares. Acta Scientiarum Naturalium Universitatis Sunyatseni. 2018;57:1-11**(in Chinese)**.
9. Wen X, Wang C, Huang C, Bai S, Zhang Q. A novel method to assess the effect of diagenesis on fossil teeth: Rare earth element signatures. J Rare Earth. 2011;29: 710-715.
10. Ferrini V, Vito CD, Mignardi S, Fucinese DV. Archaeological carved slabs of the Langobard art in churches of Peligna Valley and Spoleto (Italy): Provenance of the stones. J Archaeol Sci. 2012;39:3505-3515.
11. Wei G, Qin Y, Hu Y, Huang F, Wang C. Determining Foundry Area of Bronze Vessel Using REE in Clay Mould Residues. J Rare Earth. 2006;24:497-502.
12. Zhu J. The varieties and types of the famous inkstone in China. Stone. 2000;9:41-43**(in Chinese)**.
13. Sichuan geology and mineral resources bureau. Regional geology of sichuan province. Beijing: Geological Publishing House; 1991.p.21-37**(in Chinese)**.
14. Wang, J. Study on the Depositional system and Sequence stratigraphy of Upper Triassic-Jurassic in Sichuan basin[D]. Chengdu University of Technology, 2007**(in Chinese)**.
15. Hao, Q. Research on Provenance and Sedimentary System of the Upper Triassic Xujiahe Formantion in the Southern Sichuan Basin[D]. Chengdu University of Technology, Chengdu, 2015**(in Chinese)**.
16. Fu W, Yang M, Guo Q, Huang X, Chai M, Guo W. Micro-Structure of a Special Sericite-Jade: A Preliminary Study Using XRD and SEM Analysis. Adv Mater Res. 2013;609:503-506.

17. Ming Z, Ning J, Zhang H, Liu X. Study on Microscopic Structure and Mineral Composition of Shallow Rock Using SEM. Appl Mech 2013;303:2552-2558.
18. Liu J, Lin L Ji Y. Using Rock SEM Image to Create Pore-scale Finite Element Calculation Mesh. Phys Procedia. 2011;22:227-232.
19. Zheng, Z. Theory on autogenous grind blade and ink-making of China's She inkslab. Chin Sci Bull. 1998;17:1330-1332.
20. Li G, Wang S. A discussion on ink-making mechanism of Hongsi inkstones from Linqu, Shandong Province. Acta Petrol Et Mineral. 2016;35:175-181**(in Chinese)**.
21. Mezayen AME, Heikal MA, El-Feky MG, Shahin HA, Zeid IK, Lasheen SR. Petrology, geochemistry, radioactivity, and M–W type rare earth element tetrads of El Sela altered granites, south eastern desert, Egypt Acta Geochim. 2019;38:1-25.
22. Barca D, Larussa MF, Crisci, GM. Technological and geochemical study of two red-figured vases of unknown provenance by various analytical techniques. Appl Phys A. 2010;100:911-917.
23. Murray RW. Chemical criteria to identify the depositional environment of chert: general principles and applications. Sediment Geol. 1994;90:213-232.
24. Baziotis I, Mposkos E. Origin of metabasites from upper tectonic unit of the Lavrion area (SE Attica, Greece): Geochemical implications for dual origin with distinct provenance of blueschist and greenschist's protoliths. LITHOS. 2011;126:161-173.
25. Concepcion RAB, Dimalanta CB, Jr GPY, Faustino-Eslava DV, Queano KL, Jr RAT, et al. Petrography, geochemistry, and tectonics of a rifted fragment of Mainland Asia: evidence from the Lasala Formation, Mindoro Island, Philippines. Int J Earth Sci. 2012;101:273-290.
26. Maslov AV, Ronkin YL, Krupenin MT, Petrov GA, Kornilova AY, Lepikhina, OP, et al. Systematics of rare earth elements, Th, Hf, Sc, Co, Cr, and Ni in the vendian pelitic rocks of the Serebryanka and Sylvitsa groups from the western slope of the Central Urals: A tool for monitoring provenance composition. Geochem Int. 2006;44:559-580.
27. Cullers RL. The geochemistry of shales, siltstones and sandstones of Pennsylvanian–Permian age, Colorado, USA: implications for provenance and metamorphic studies. LITHOS. 2000;51:181-203.
28. Yang S, Li C. Research progress in REE tracer for sediment source. Advance in earth Sci. 1999;14:63-66**(in Chinese)**.
29. Zhao Z. Principles of Trace Element Geochemistry. Beijing: Science Press; 1997**(in Chinese)**.
30. Liang F, Huang W, Niu, J, Campus K. Provenance Analysis of Permain Shan1 and He 8 Formation in Permian in Southwest Ordos Basin. Acta Sedimentologica Sinica. 2018;1:142-153**(in Chinese)**.
31. Zaremotlagh S, Hezarkhani A, Sadeghi M. Detecting homogenous clusters using whole-rock chemical compositions and REE patterns: A graph-based geochemical approach. J Geochem Explor. 2016;170:1-52.
32. Shields G, Stille P. Diagenetic constraints on the use of cerium anomalies as palaeoseawater redox proxies: an isotopic and REE study of Cambrian phosphorites. Chem Geol. 2001;175:29-48.

33. Li S, Yang X, Sun W. Ages and zircon Hf isotope geochemistry of the Dengjiawu Mo deposit in Shexian, South Anhui Province. Acta Petrologica Sinica. 2012;12: 3980-3992**(in Chinese)**.
34. Chen Z, He X, Lu Y, Yu H. Geochemical characteristics of trace elements of the Duanxi Inkstone. Geochimica. 2011;40:387-391**(in Chinese)**.
35. Sako, A. Chapter 7 Geochemical cycling of trace and rare earth elements in Lake Tanganyika and its major tributaries. Developments in Environ Sci. 2007;5:135-171.
36. Taylor SR, Mclennan SM, Armstrong RL, Tarney J. The Composition and Evolution of the Continental Crust: Rare Earth Element Evidence from Sedimentary Rocks [and Discussion]. Philos T R Soc A. 1981;301:381-399.
37. Bhatia MR, Crook AWK. Trace element characteristics of graywackes and tectonic setting discrimination of sedimentary basins. Contrib Mineral Petr. 1986;92:181-193.
38. Haskin LA, Wildeman TR, Haskin MA. An accurate procedure for the determination of the rare earths by Neutron activation. J of Radioanal Ch. 1968;1:337-348.
39. Oliveira SMB, Larizzatti FE, Favaro DIT, Moreira SRD, Piovano EL. Rare earth element patterns in lake sediments as studied by neutron activation analysis. J Radioanal Nucl Ch. 2003;258:531-535.
40. Shen J, Liu J. REE Geochemical characteristics of the two types of granitic rocks in Jiangxi province and their metallogenic significance. Geochimica. 1986;3:235-250**(in Chinese)**.
41. She L, Qin Y, Luo W, Huang F, Li T. Provenance-tracing of Turquoise in Northwest Hubei Using Rare Earth Elements. Chi Rare Earth. 2009;30:59-62**(in Chinese)**.
42. Hegde VS, Chavadi VC. Geochemistry of late Archaean metagreywackes from the Western Dharwar Craton, South India: Implications for provenance and nature of the Late Archaean crust. Gondwana Res. 2008;15:178-181.

Figures

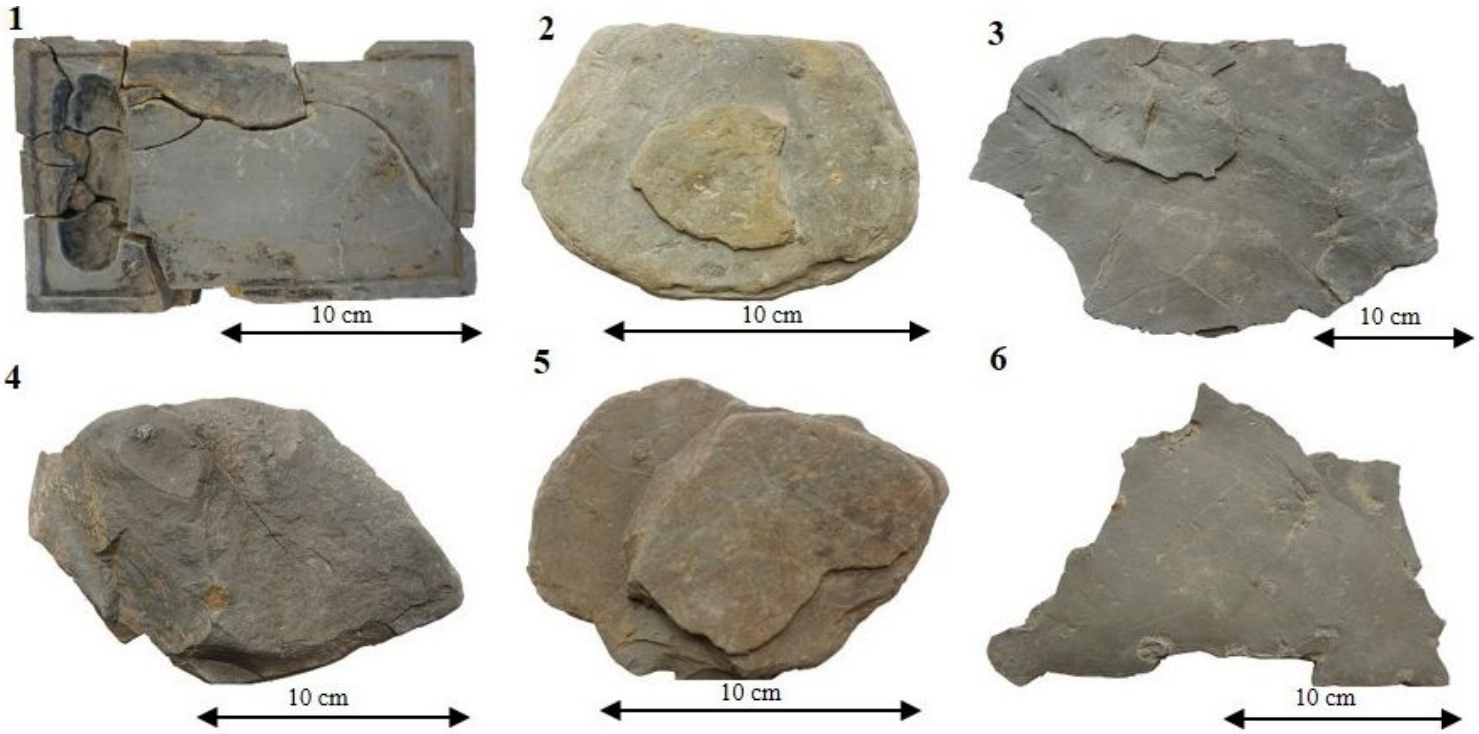

Figure 1

Images of relics sample (1) and control samples (2, 3, 4, 5, 6)

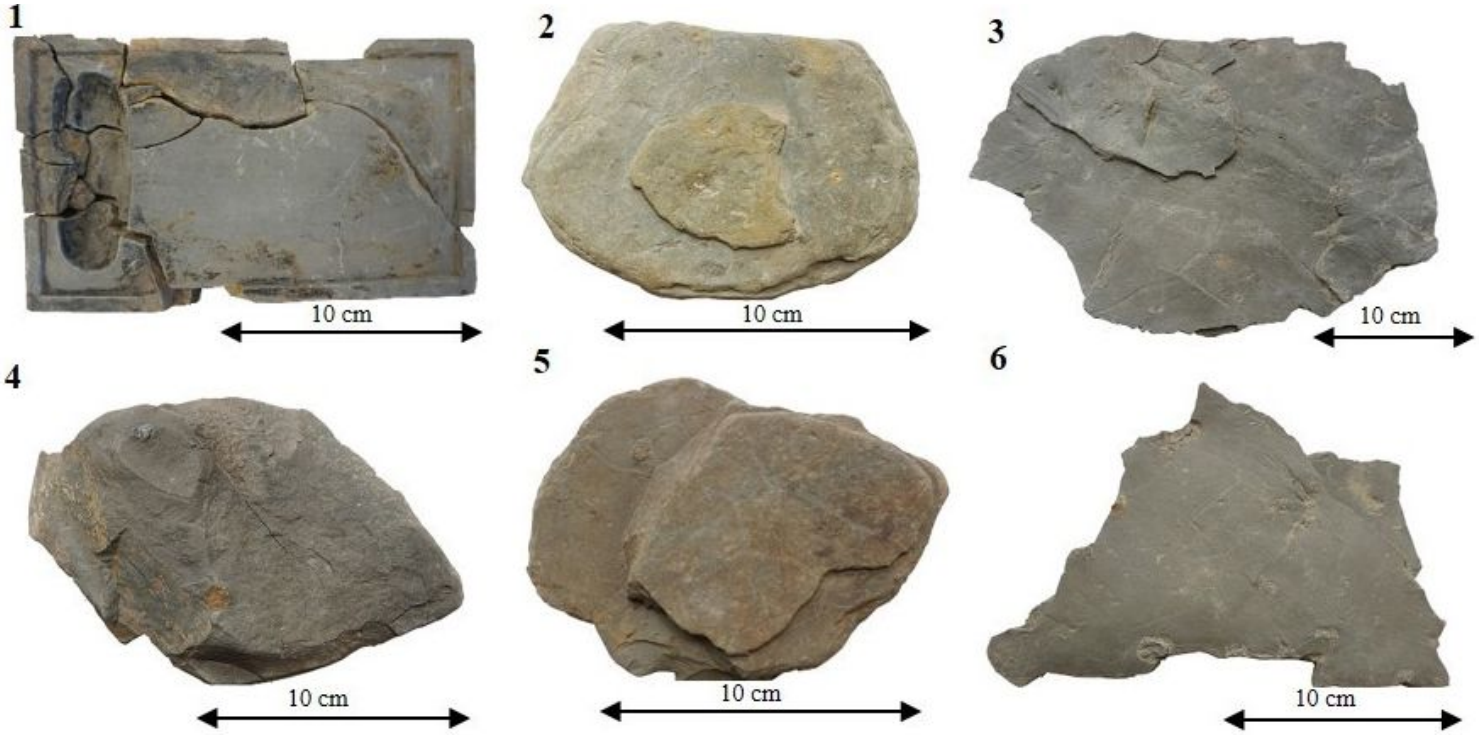

Figure 1

Images of relics sample (1) and control samples (2, 3, 4, 5, 6)

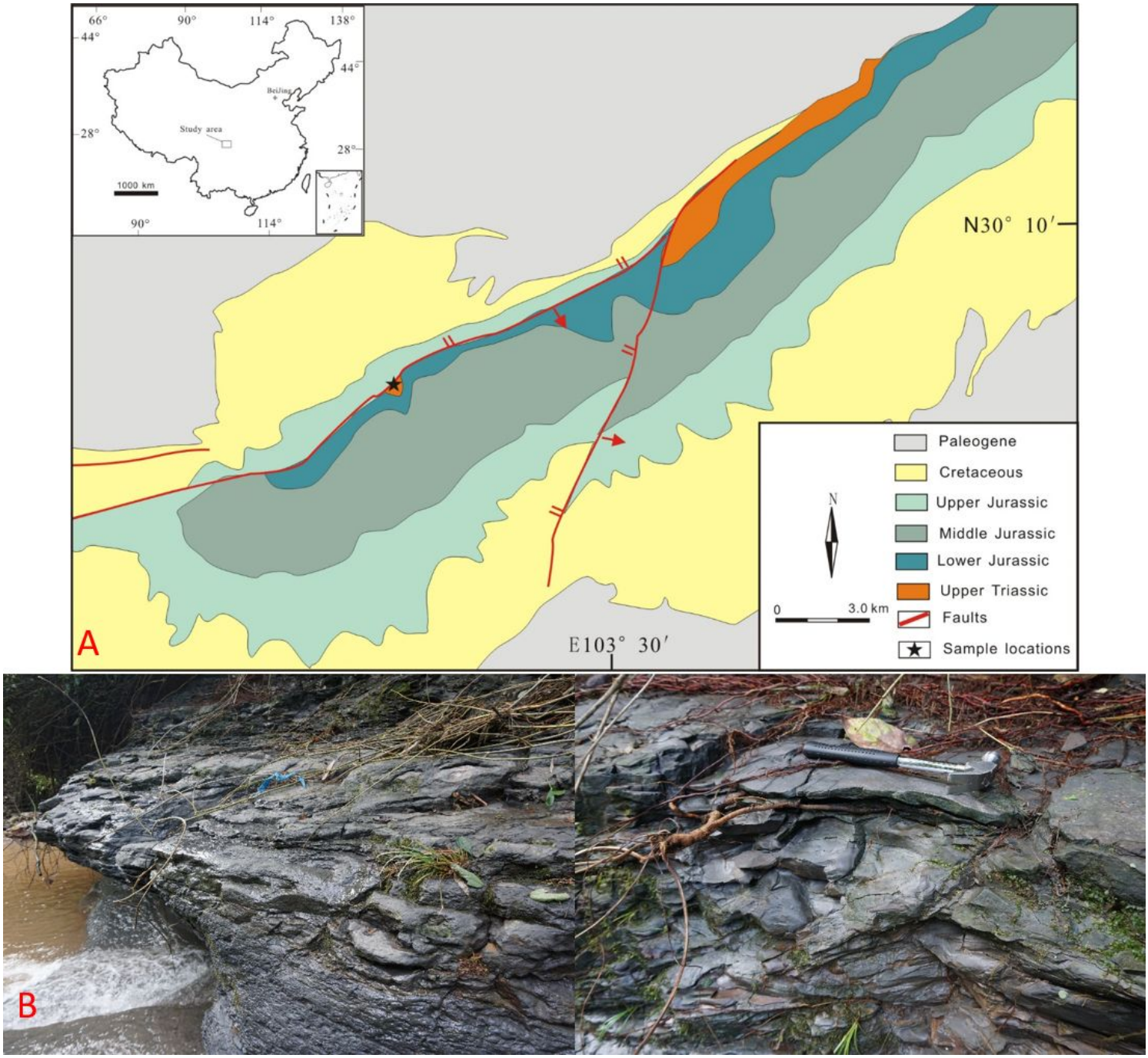

Figure 2

(A) Simplified geological image of the Pujiang County; (B) Partial field sampling images Note: The designations employed and the presentation of the material on this map do not imply the expression of any opinion whatsoever on the part of Research Square concerning the legal status of any country, territory, city or area or of its authorities, or concerning the delimitation of its frontiers or boundaries. This map has been provided by the authors.

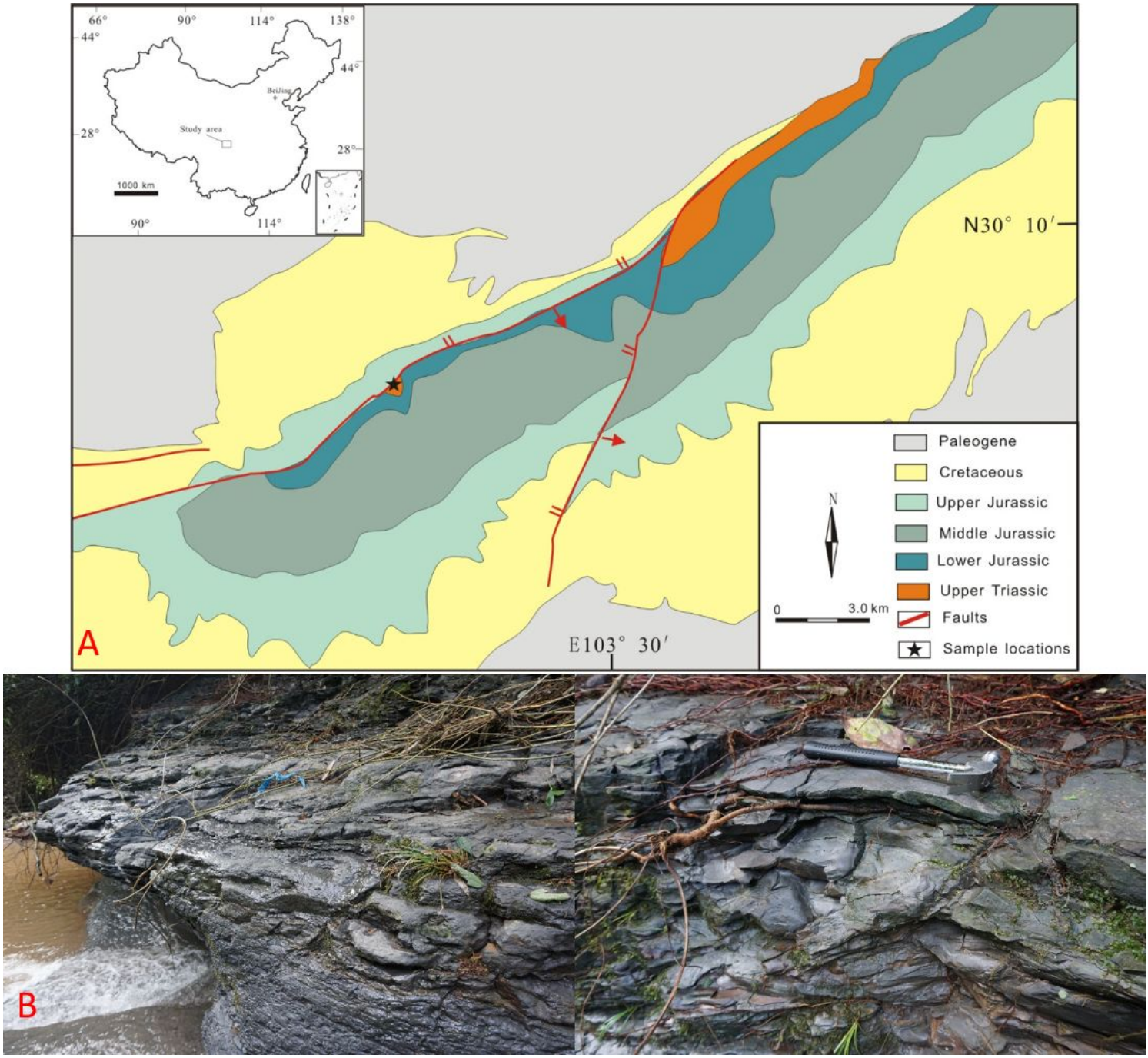

Figure 2

(A) Simplified geological image of the Pujiang County; (B) Partial field sampling images Note: The designations employed and the presentation of the material on this map do not imply the expression of any opinion whatsoever on the part of Research Square concerning the legal status of any country, territory, city or area or of its authorities, or concerning the delimitation of its frontiers or boundaries. This map has been provided by the authors.

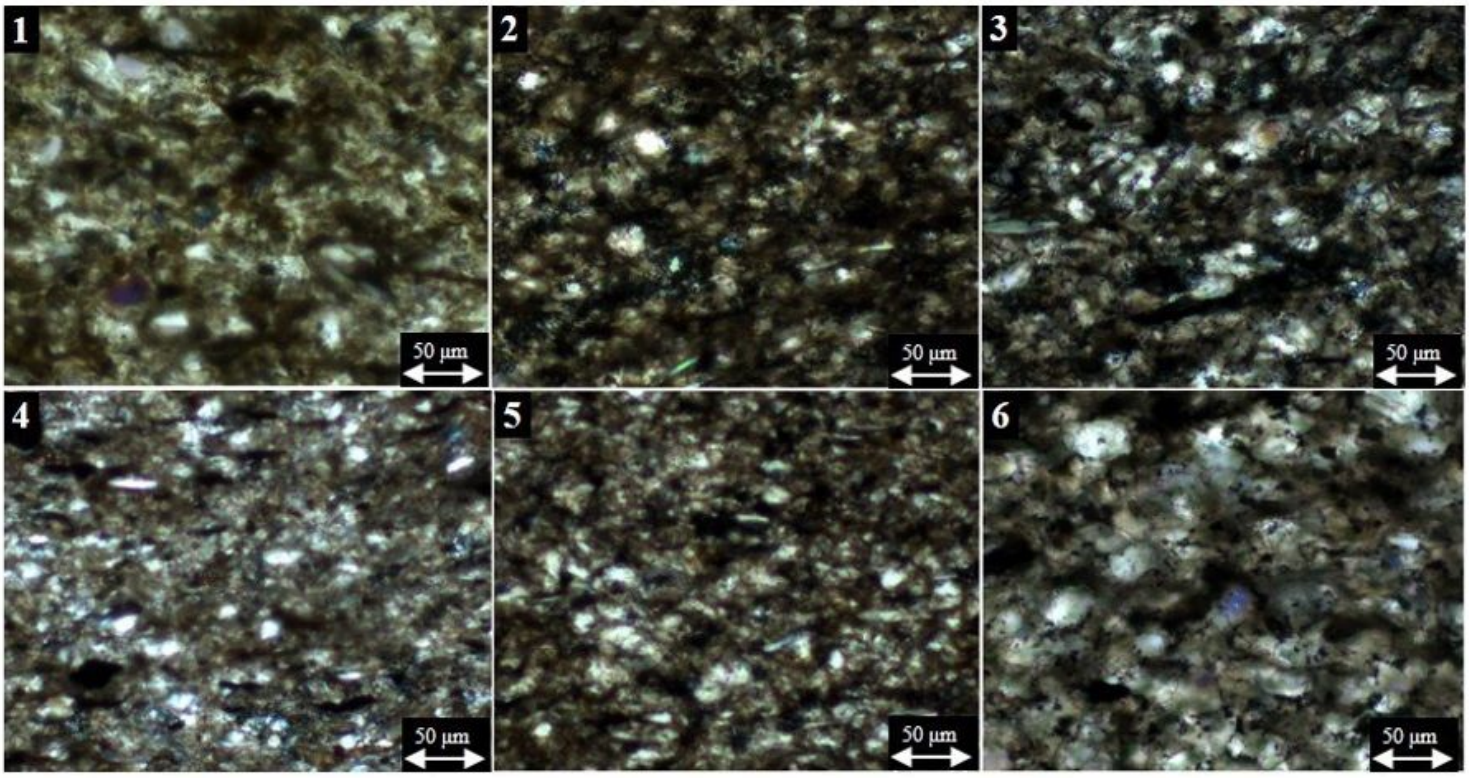

Figure 3

Polarization images of relics sample (1) and control samples (2, 3, 4, 5, 6)

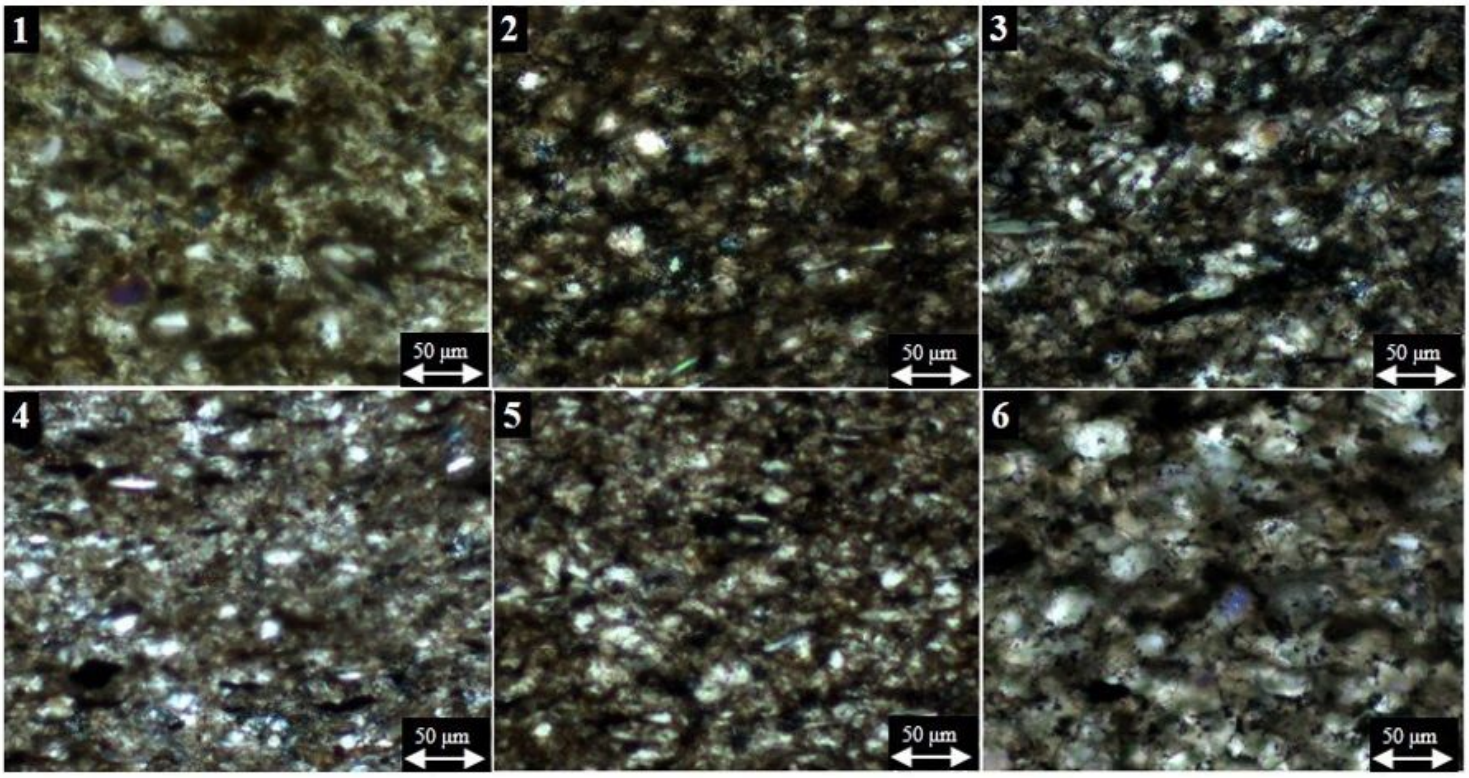

Figure 3

Polarization images of relics sample (1) and control samples (2, 3, 4, 5, 6)

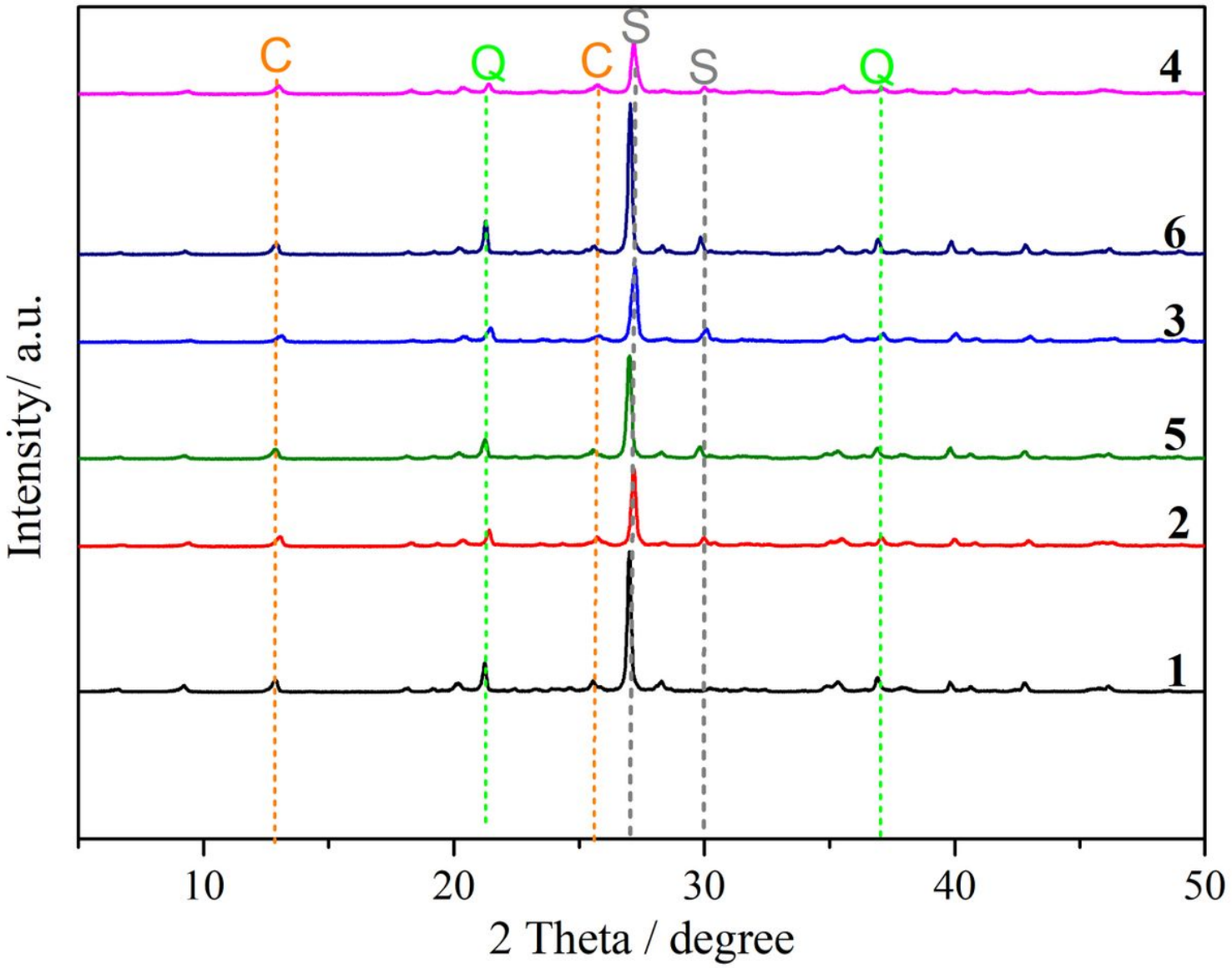

Figure 4

The XRD patterns of the relics sample (1) and control samples (2, 3, 4, 5, 6) (S-sericite, C-chlorite, Q-quartz)

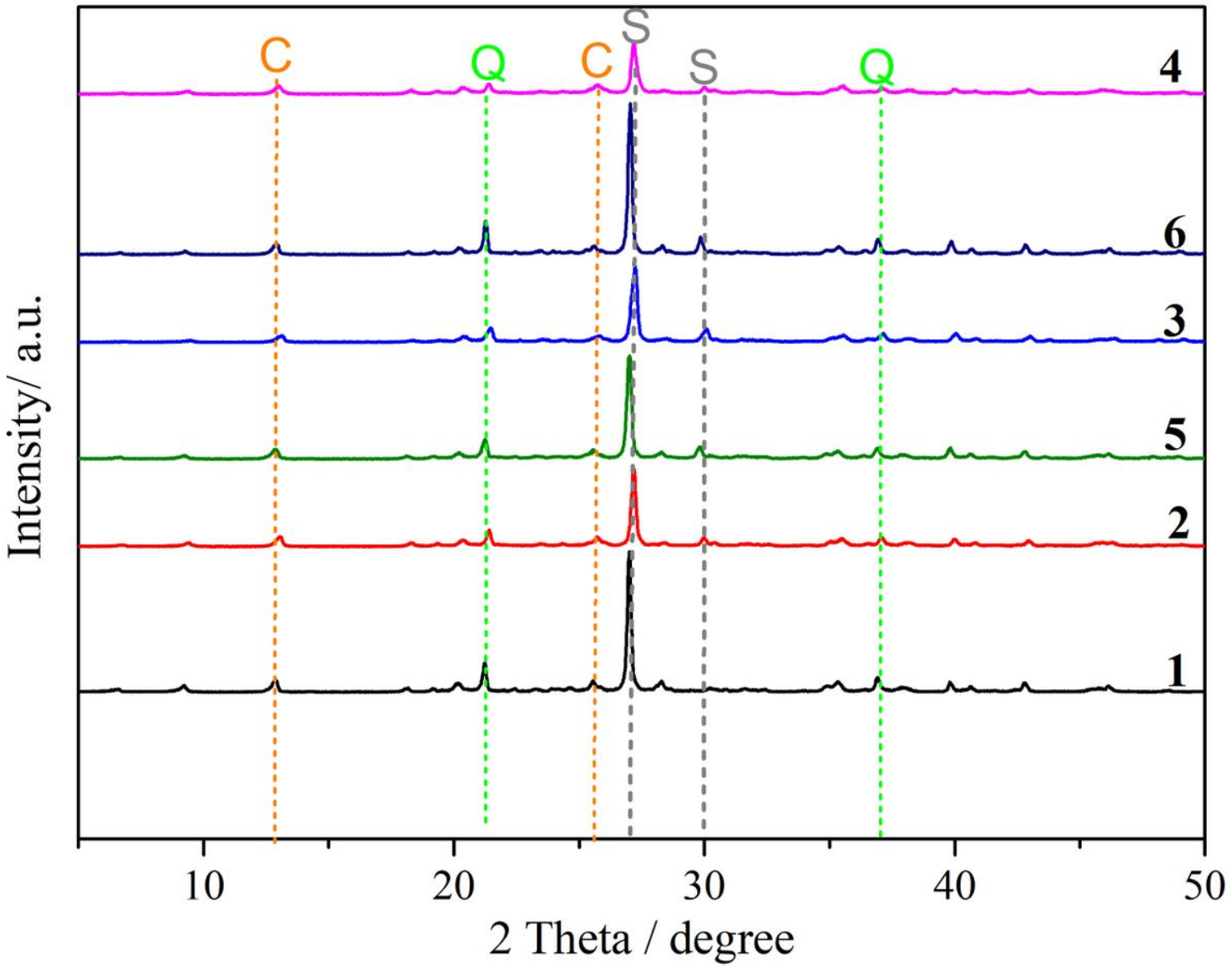

Figure 4

The XRD patterns of the relics sample (1) and control samples (2, 3, 4, 5, 6) (S-sericite, C-chlorite, Q-quartz)

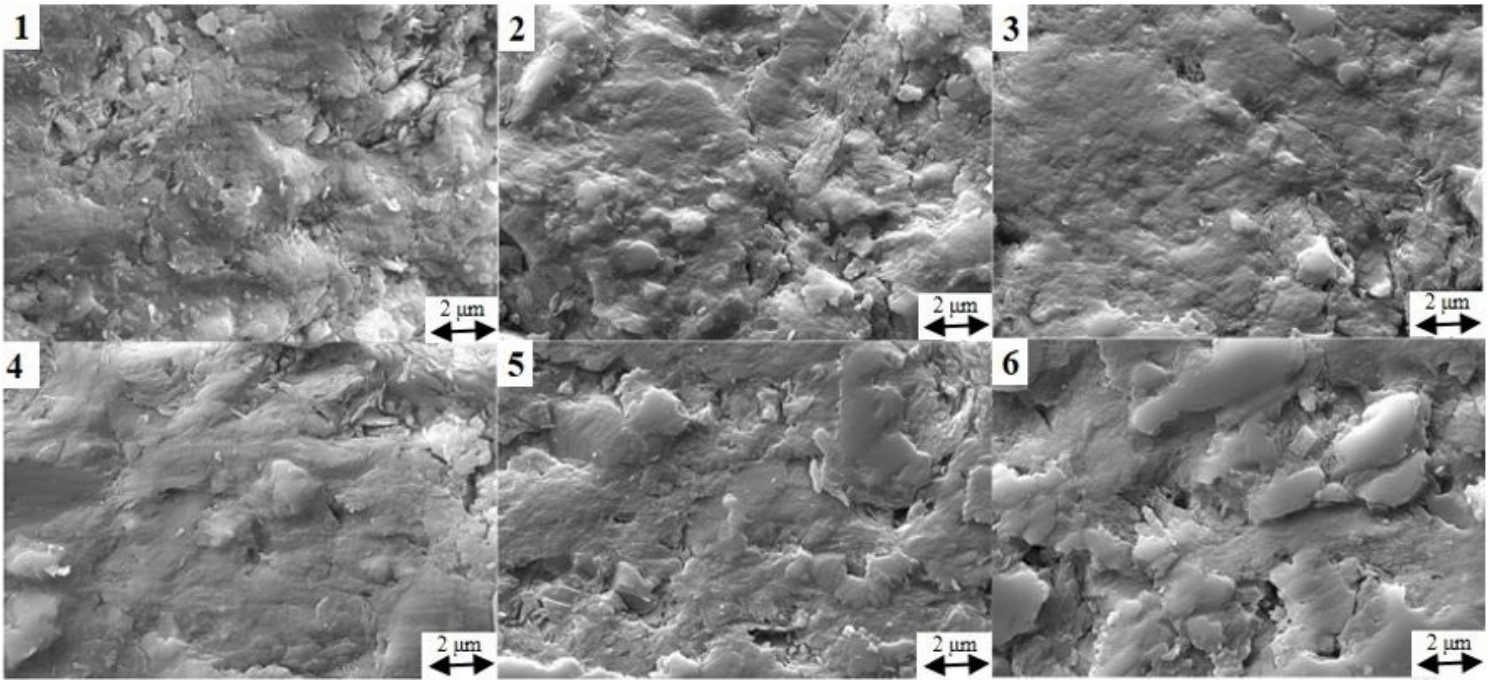

Figure 5

SEM images of relics sample (1) and control samples (2, 3, 4, 5, 6)

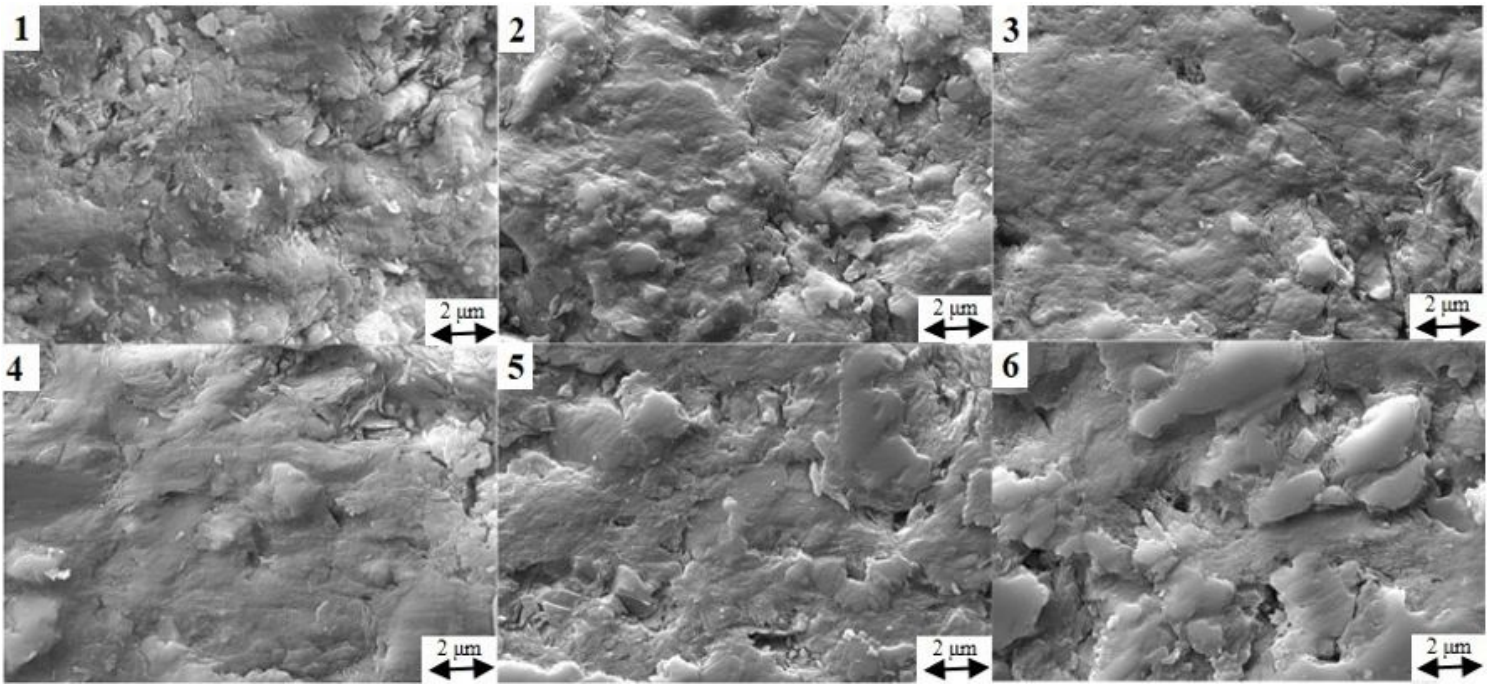

Figure 5

SEM images of relics sample (1) and control samples (2, 3, 4, 5, 6)

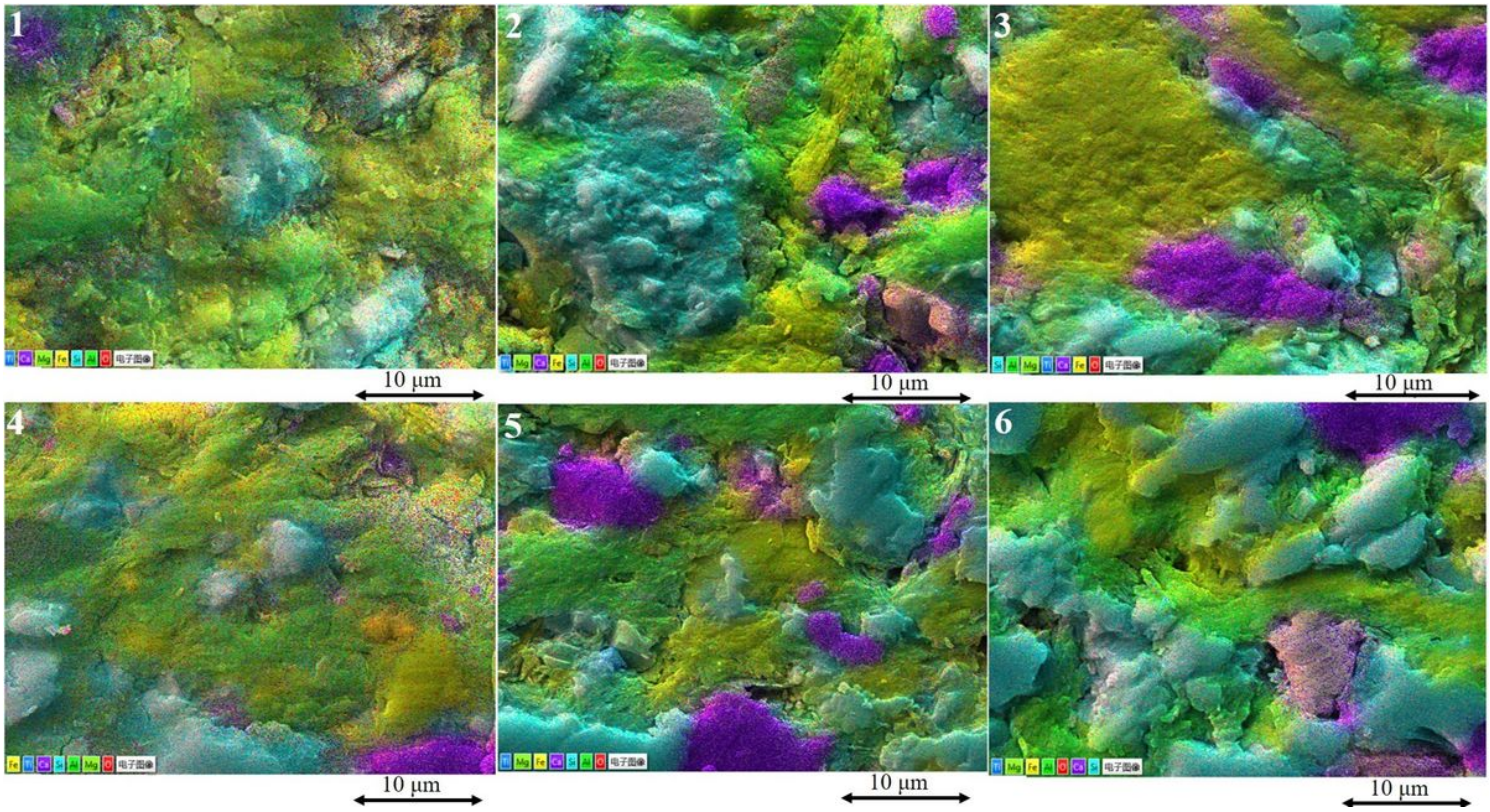

Figure 6

EDS images of relics sample (1) and control samples (2, 3, 4, 5, 6)

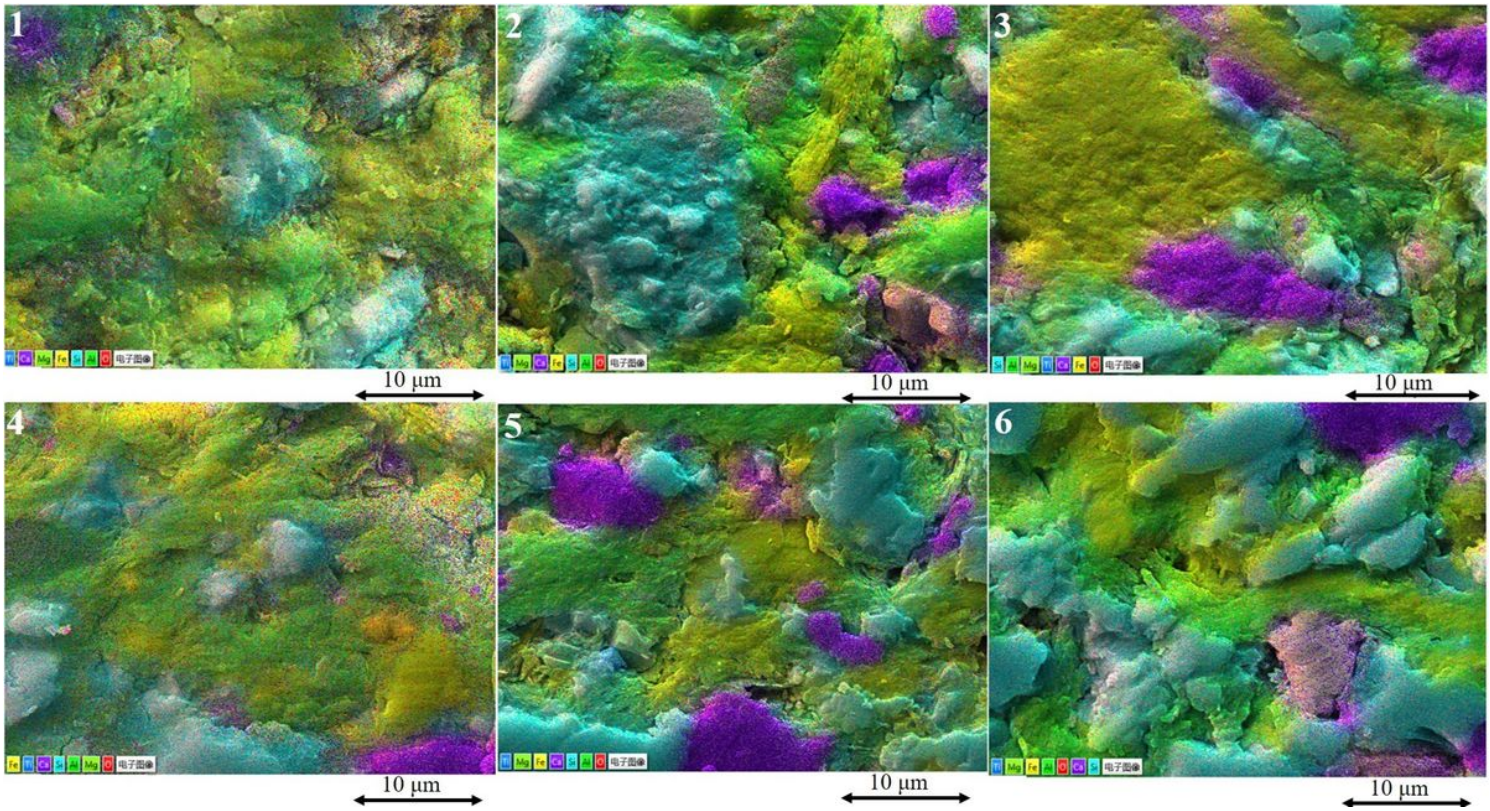

Figure 6

EDS images of relics sample (1) and control samples (2, 3, 4, 5, 6)

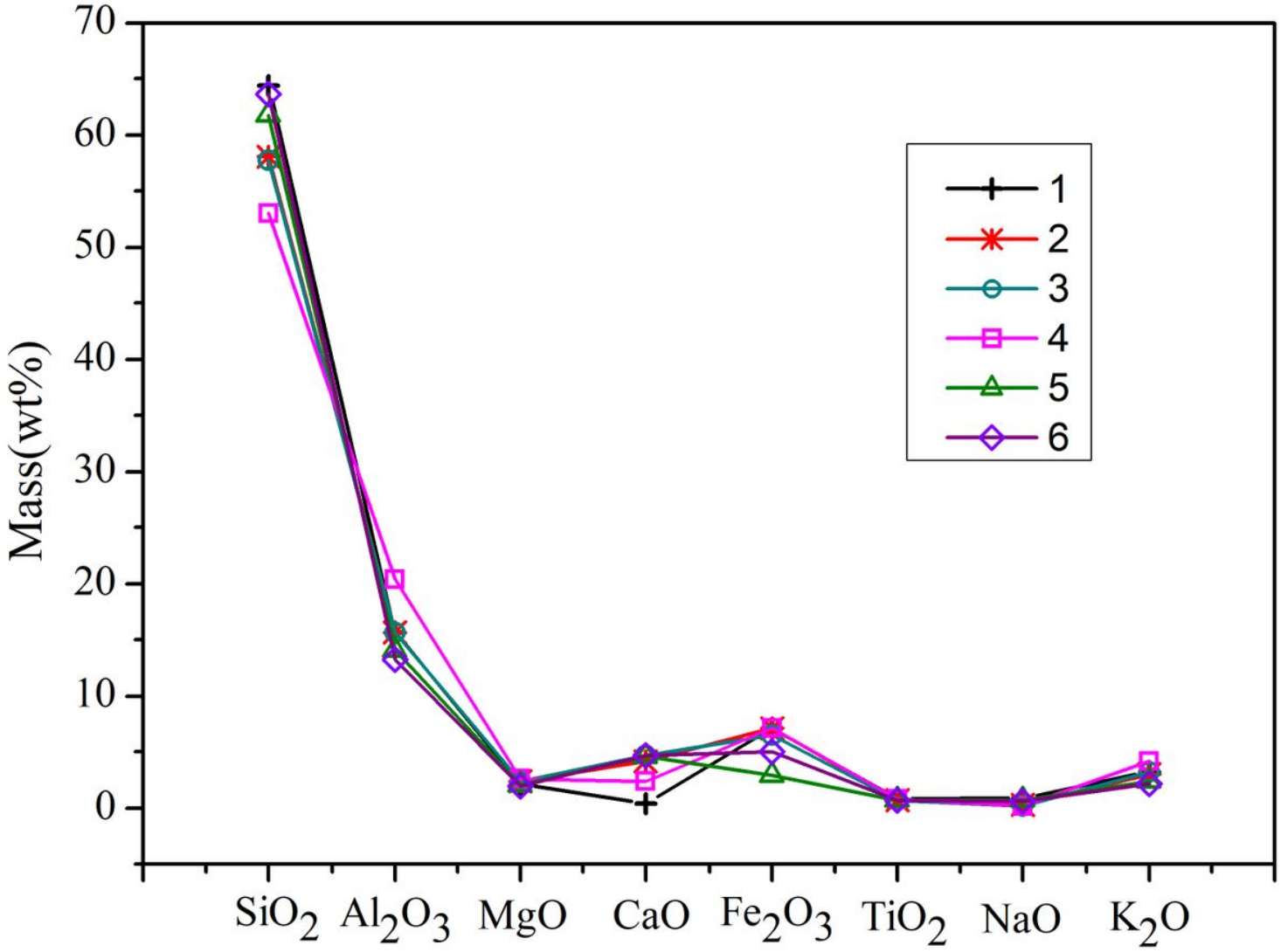

Figure 7

The patterns of the Major elements of the relics sample (1) and control samples (2, 3, 4, 5, 6)

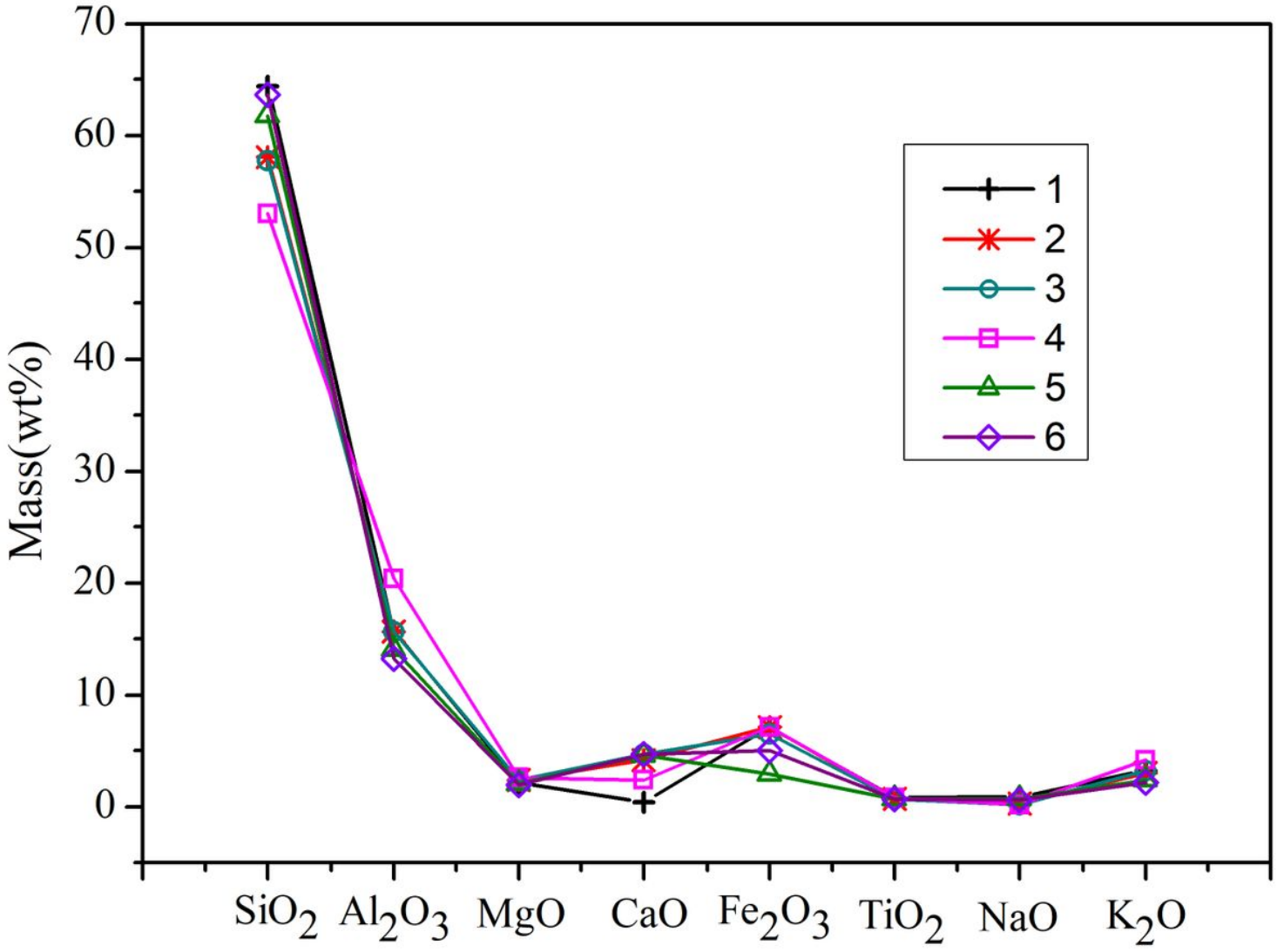

Figure 7

The patterns of the Major elements of the relics sample (1) and control samples (2, 3, 4, 5, 6)

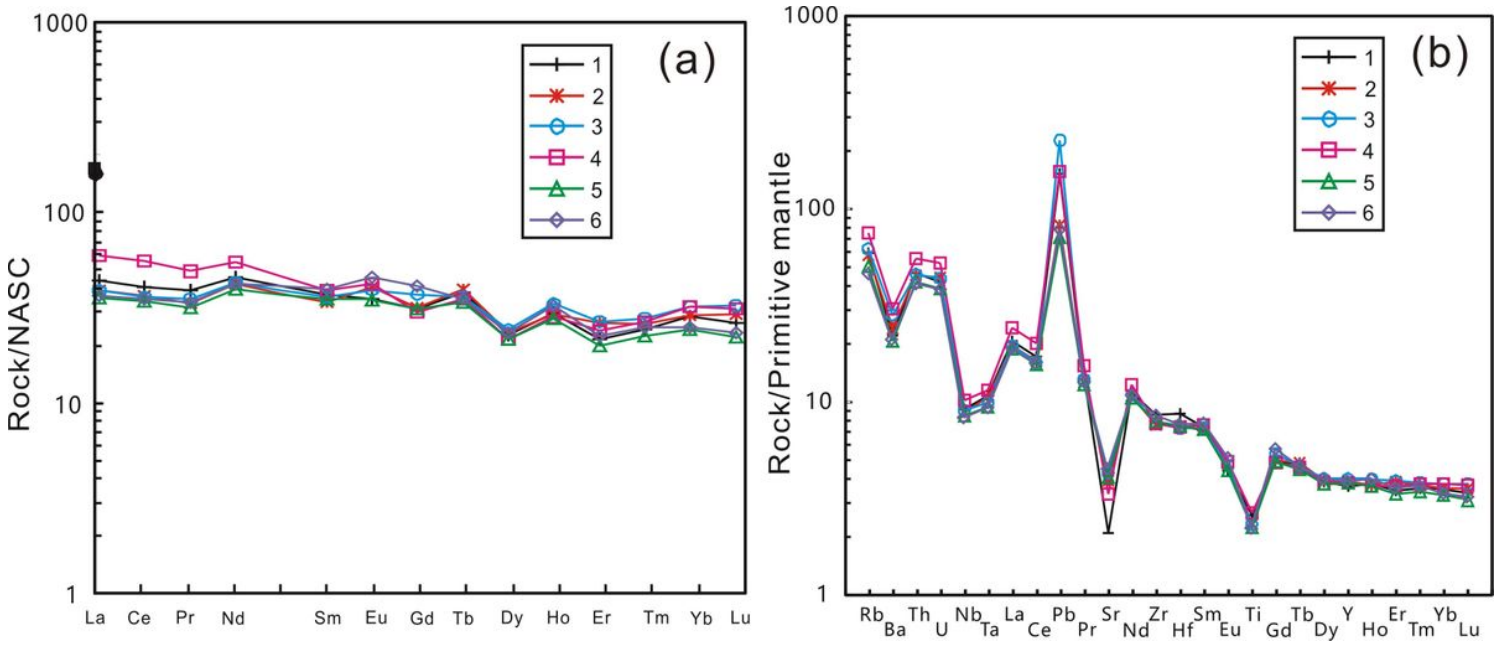

Figure 8

(a) The standardized distribution patterns of REE in NASC of relics sample (1) and control samples (2, 3, 4, 5, 6). (b) The primitive-mantle-normalized trace element spider diagram of relics sample (1) and control samples (2, 3, 4, 5, 6)

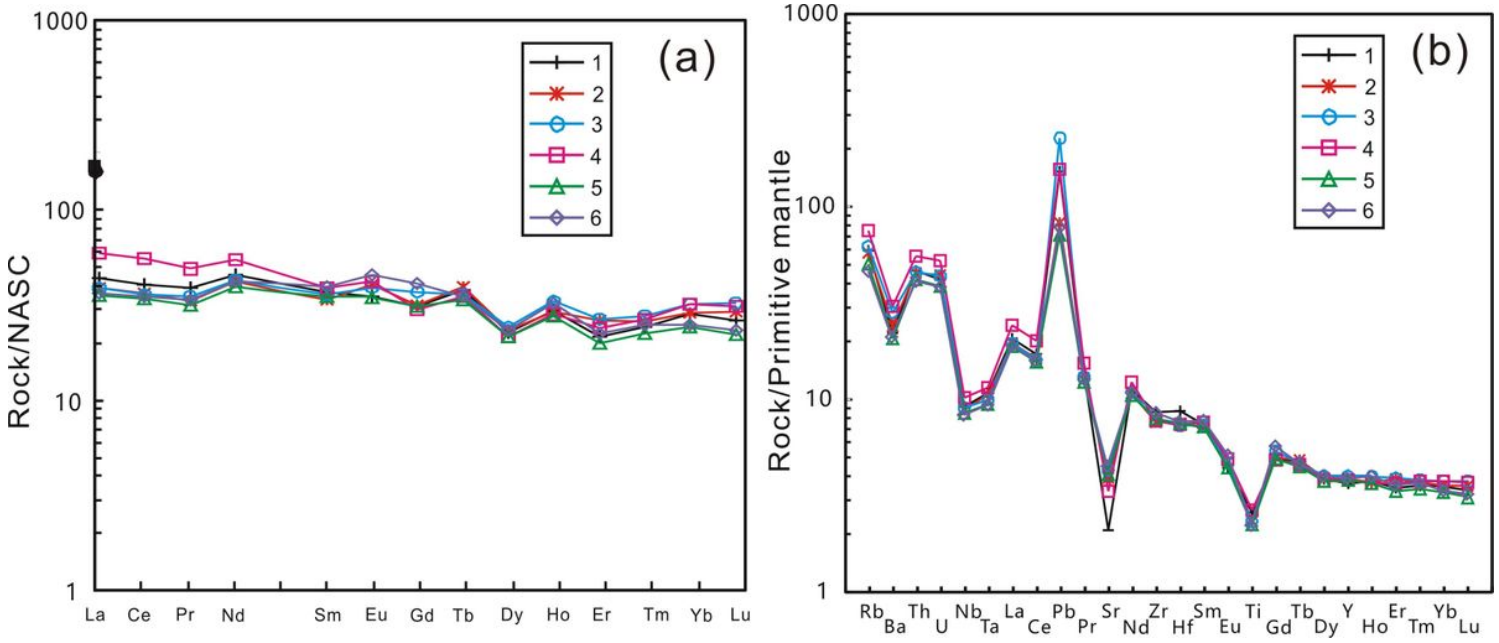

Figure 8

(a) The standardized distribution patterns of REE in NASC of relics sample (1) and control samples (2, 3, 4, 5, 6). (b) The primitive-mantle-normalized trace element spider diagram of relics sample (1) and control samples (2, 3, 4, 5, 6)

Supplementary Files

This is a list of supplementary files associated with this preprint. Click to download.

- GraphicalAbstract.docx
- GraphicalAbstract.docx